

CHARACTERISTICS OF A STABILIZED ARC IN A CHANNEL  
WITH A DISTRIBUTED GAS FEED

G. M. Mustafin

The characteristics of an electric arc in a sectional channel with a distributed gas feed are investigated. The good prospects of using such channels as an interelectrode insert in plasmatrons are shown in [1, 2].

Volt-ampere and thermal characteristics of the arc in a wide range of lengths of the insert are obtained. The distributions of potential and electric field of the arc in the insert region are investigated. It is shown that the insert can increase the arc voltage and mean mass stagnation enthalpy of the heated gas by a factor of two or three in comparison with an ordinary two-chamber plasmatron.

**Notation.**  $U, V$  - arc voltage;  $I, a$  - arc current,  $V, V$  - arc potential;  $a$ , cm - length of insert;  $E, V \cdot \text{cm}^{-1}$  - longitudinal component of electric field in arc;  $\langle E \rangle, V \cdot \text{cm}^{-1}$  - mean value of  $E$  in insert region;  $G, \text{g} \cdot \text{sec}^{-1}$  - air flow rate through arc chamber;  $d_a, d, d_c$ , cm - internal diameters of anode, insert, and cathode, respectively;  $r, z$ , cm - cylindrical coordinates;  $Q_1, Q_2, Q_3$ , kW - amounts of heat removed from inside electrode, insert, and outlet electrode, respectively, in 1 sec;  $\eta$  - thermal efficiency of plasmatron;  $\eta_1, \eta_2, \eta_3$  - values of  $Q_1, Q_2, Q_3$  as % of arc power;  $T, ^\circ\text{K}$  - mean-mass stagnation temperature of gas flow at plasmatron outlet;  $\Delta h, \text{kJ/kg}$  - mean-mass stagnation enthalpy of gas flow in same conditions.

**1. Experimental Apparatus.** For the arc investigation we used the plasmatron illustrated schematically in Fig. 1a. The water-cooled copper electrode 1, the outlet electrode 2, and the insert sections 3, insulated from one another and from the electrodes, form the arc chamber of the plasmatron. The polarity of connection of the electrodes was reversed, i.e., the outlet electrode was the cathode. The gas was discharged into the atmosphere. The pressure in the arc chamber in the region between the anode and first section of the insert was 2-4 atm, depending on the parameters of the plasmatron.

The experiments were conducted with  $d_c=1.4$  cm,  $d=1$  cm, and  $d_a=1.2$  cm. The lengths of the inside and outlet electrodes were 17.2 and 6 cm, respectively. For comparison of the characteristics we also carried out experiments on a two-chamber plasmatron with a smooth outlet electrode. In this case the length of the outlet electrode was 30 cm. The length of the insert varied from 18 to 43 cm. The sections of the insert were of different thicknesses and were arranged along the insert in groups in order of de-

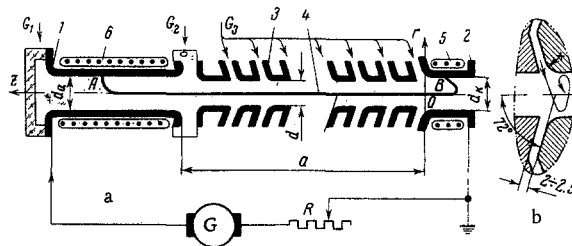


Fig. 1. Diagram of plasmatron.

Novosibirsk. Translated from Zhurnal Prikladnoi Mekhaniki i Tekhnicheskoi Fiziki, Vol. 9, No. 4, pp. 124-129, July-August, 1968. Original article submitted January 26, 1968.

© 1972 Consultants Bureau, a division of Plenum Publishing Corporation, 227 West 17th Street, New York, N. Y. 10011. All rights reserved. This article cannot be reproduced for any purpose whatsoever without permission of the publisher. A copy of this article is available from the publisher for \$15.00.

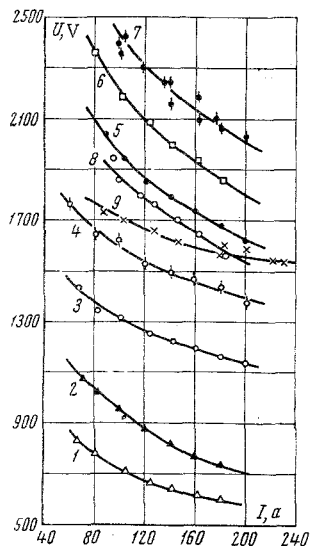


Fig. 2. U-I characteristics of arc: 3)  $a=18.8$  cm; 4)  $a=23.2$  cm; 5 and 9)  $a=33$  cm; 6)  $a=38$  cm; 7 and 8)  $a=43$  cm.

were determined by RS-5, RS-7, and RED model No. 3101 rotameters. The arc voltage and current were measured with an M366 voltmeter of accuracy class 1.0 and an LM-1 instrument of accuracy class 0.5. The potentials of the insulated sections relative to the cathode were measured with S-50 electrostatic voltmeters (1- and 3-kV scales) of accuracy class 1.0 and an S-95 voltmeter (1.5-kV scale) of accuracy class 1.5.

The experiments showed that the aerodynamics of the gas flow entering the intersectional gaps had a considerable effect on stabilization of the arc and the breakdown voltage between the arc and wall of the insert section. In [1] the intersectional gaps were perpendicular to the plasmatron axis. In this work the gaps between the sections were at an angle of  $72^\circ$  to the axis and the opening from the gap into the channel was smoothed off in the direction of the flow (Fig. 1, b). This ensured smoother flows, led to stable operation of the plasmatron, and enabled us to carry out investigations of the arc in a significantly larger range of lengths. In addition, the intersectional insulators were shielded from radiation. Replacement of the inside end-face electrode used in [1] by a hollow cylindrical type and the application of magnetic fields to the end regions of the arc enables us to operate the plasmatron for long periods without significant erosion of the electrodes.

**2. Volt-Ampere and Thermal Characteristics.** Figure 2 shows U-I characteristics obtained for insert lengths varying from 18 to 43 cm (curves 3-9). For comparison the same figure shows the U-I characteristics of a two-chamber plasmatron with a smooth outlet electrode (curves 1, 2). Curves 1 and 8 correspond to  $G=10 \text{ g} \cdot \text{sec}^{-1}$ , and the others to  $G=15 \text{ g} \cdot \text{sec}^{-1}$ . The figures show that an increase in the length of the insert with a distributed feed of gas into the intersectional gaps can lead to a considerable increase in the arc voltage. For instance, curves 2 and 7 in Fig. 2 show that when  $I=180 \text{ a}$  the arc voltage in a plasmatron with an insert is approximately 2.8 times greater than the arc voltage in a plasmatron without an insert.

As distinct from the data of [1], the U-I characteristics are descending. One of the possible reasons for the descending U-I characteristics is shunting of the arc in the inside electrode. To determine the role of shunting we conducted an experiment with an end-face inside electrode (curve 9, Fig. 2). A comparison of curves 5 and 9 shows that in the latter case the arc voltage and the steepness of the U-I characteristic are slightly reduced, but the characteristic is still descending. The cause of formation of a characteristic of this form will be considered below.

creasing thickness in the direction of the gas flow. This was dictated by the reduction in breakdown potential between the arc column and the sections in the direction of flow due to the reduction of thickness of the layer of cold gas in the breakdown gap. In the experiments we used sections 2, 1.5, and 1 cm thick.

Air was admitted at flow rate  $G_1$  into the inside electrode through two tangential orifices of diameter 1.2 mm at a distance of 2.5 cm from the plasmatron axis. The flow  $G_2$  entered the arc chamber through four tangential orifices of diameter 1.5 mm at a distance of 4.5 cm from the plasmatron axis. The flow  $G_3$  entered the inter-sectional spaces through vortex rings and was distributed through the inter-sectional gaps of width 2-2.5 mm along the arc chamber, as shown in Fig. 1, a and b.

The inter-sectional vortex rings each had two tangential orifices 0.8 mm in diameter at a distance of 2.0 cm from the plasmatron axis.

The total air flow rate  $G=G_1+G_2+G_3$  varied from 10 to 20  $\text{g} \cdot \text{sec}^{-1}$ . The flow rates  $G_1:G_2:G_3$  were in the ratio 1:4.1:7.4.

The plasmatron was started by means of a wire. After ignition the arc 4 occupied the position AB. Movement of the arc spots A and B over the inside cylindrical surfaces of the anode 1 and cathode 2 was secured by the vortical motion of the gas through the chamber and by the magnetic fields of solenoids 5 and 6.

The temperature of the cooling water was measured by mercury thermometers with  $0.5^\circ \text{C}$  scale divisions. The water and air flow rates

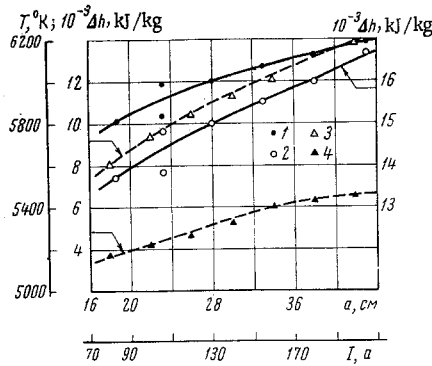


Fig. 3

Fig. 3. Stagnation temperature and mean-mass enthalpy as functions of  $I, a$ ; the arrows indicate to which vertical axis the curve corresponds; points 1 and 2 for  $I=180, G=10$ , points 3 for  $a=33, G=16$ , points 4 for  $G=15$ .

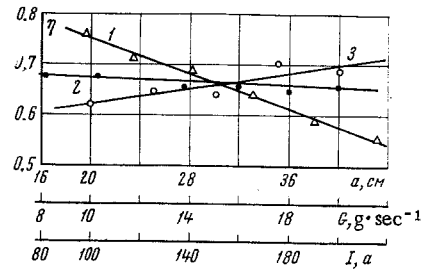


Fig. 4

Fig. 4. Efficiency of plasmatron as function of insert length (curve 1 for  $I=180, G=15$ ), arc current (curves 2 for  $a=33, G=15$ ), and gas flow rate (curve 3 for  $I=180, a=33$ ).

As Fig. 2 shows, the arc voltage depends significantly on the gas flow rate through the arc channel. For instance, a comparison of curves 7 and 8 shows that for current  $I=180$  a an increase in the flow rate by a factor of 1.5 (from 10 to 15  $g \cdot sec^{-1}$ ) leads to an increase in the arc voltage in a plasmatron with an insert by 490 V, whereas for a two-chamber plasmatron with a smooth outlet electrode (curves 1 and 2) in the same conditions the voltage increase is only 135 V.

As is known, in an ordinary plasmatron with a self-adjusting arc an increase in the gas flow rate leads to an increase in the arc length and the electric field in the region of the column situated along the channel axis. These two effects help to increase the arc voltage. In a plasmatron with an insert the length of the arc is practically independent of the gas flow rate and, hence, the increase in  $U$  with increase in  $G$  is due to increase in the electric field of the arc. Since the arc is longer in a plasmatron with an insert than in an ordinary plasmatron, then even a small increase in the electric field leads to a large increase in  $U$  of the arc. In addition, at the outlet end of the arc, as will be shown below, the electric field is fairly high and depends significantly on the gas flow rate.

The arc in an ordinary plasmatron is relatively short and in the investigated range of parameters the high-temperature arc plasma occupies only a small region near the channel axis, and the bulk of  $G$  flows past the arc without being heated to a high temperature. This, in particular, explains the relatively small increase in the voltage of the self-adjusting arc with increase in the gas flow rate. In a plasmatron with an insert the high-temperature part of the flow occupies a larger region, i. e., a larger part of  $G$  interacts with the arc. This accounts for the great increase in  $U$  with increase in  $G$  in a plasmatron with an insert.

With  $a \geq 33$  cm the  $U-I$  characteristics were recorded also for the case of direct polarity. Within the limits of measurement error at currents of 100-200 a they coincided with the  $U-I$  characteristics of the arc in the case of reversed polarity. This is an important property of the  $U-I$  characteristics of the arc in a plasmatron with an insert and indicates that with long inserts and high currents the arc has an almost constant length.

TABLE 1

$a, cm$	$U, V$	$Q_1, kW$	$Q_2, kW$	$Q_3, kW$	$\eta_1, \%$	$\eta_2, \%$	$\eta_3, \%$
18.8	975	5.57	27.27	15.22	3.15	15.43	8.61
28	1230	5.06	50.36	20.09	2.27	22.63	9.03
33	1365	5.09	69.05	20.57	2.06	27.96	8.33
38	1530	5.64	91.27	22.75	2.04	32.98	8.22

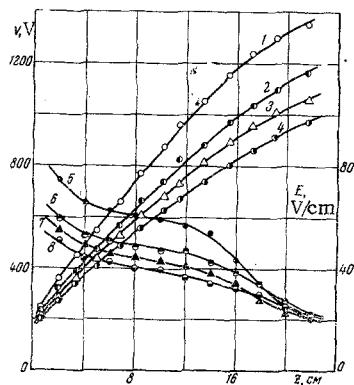


Fig. 5

Fig. 5. Distributions of  $V$  (curves 1, 2, 3, 4) and  $E$  (curves 5, 6, 7, 8) in insert region,  $a=23.2$  cm;  $I=100$  a for curves 1, 5, 3, 7;  $I=180$  a for curves 2, 6, 4, 8;  $G=15$  for curves 1, 5, 2, 6;  $G=10$  for curves 3, 7, 4, 8.

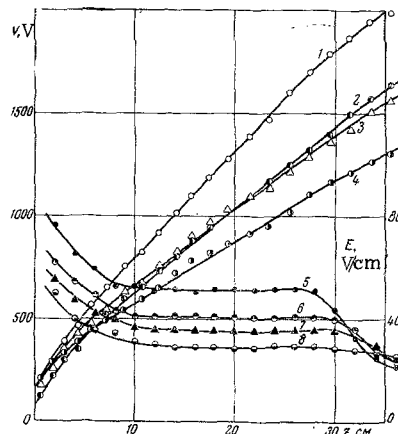


Fig. 6

Fig. 6. Distributions of  $V$  (curves 1, 2, 3, 4) and  $E$  (curves 5, 6, 7, 8) in insert region,  $a=38$  cm; the parameters of the curves are the same as in Fig. 5.

The mean-mass stagnation temperature of the heated gas at the plasmatron outlet is shown as a function of the insert length in Fig. 3 (curve 1). This figure shows that for a given current the rate of increase in the mean-mass temperature of the emerging gas decreases with increase in the insert length. The obtained relationship  $T(z)$  depends on the integral energy balance of the plasmatron and the relationship between the enthalpy of the gas and its temperature.

The increase in the mean-mass stagnation enthalpy in relation to the insert length is represented by curve 2. It can be seen that even in the case of long inserts  $\Delta h$  continues to increase. This indicates the effectiveness of the insert as a means of obtaining a gas flow with high enthalpy. The slowing-down of the temperature increase revealed by Fig. 3 is due to the well-known typical variation of the enthalpy of air with temperature.

Curves 3 and 4 in Fig. 3 respectively represent the relationships  $\Delta h(I)$  for plasmatrons with an insert and an ordinary two-chamber plasmatron with a smooth outlet electrode. In the investigated range of  $I$  the increase  $\Delta h$  with increase in current is greater in a plasmatron with an insert than in an ordinary plasmatron, and its absolute value is higher. For instance, curves 3 and 4 in Fig. 3 show that for  $I=200$  a  $\Delta h$  for a plasmatron with an insert is more than twice  $\Delta h$  for a plasmatron without an insert.

Figure 4 shows plots of the efficiency of a two-chamber plasmatron with an insert against the insert length, the arc current, and the total air flow rate. As was to be expected, the efficiency decreases with increase in the insert length and increases with increase in the flow rate.

A special feature of this plasmatron is that in the investigated range of parameters its efficiency is independent of the current.

We can surmise that the obtained relationship  $\eta(I)$  depends significantly on the nature of the gas flow in the wall region of the channel of the investigated plasmatron.

An analysis of the  $U-I$  characteristics and the obtained relationships  $\eta(I)$  show that further increase in  $T$  is possible only if the arc current or insert length is increased.

It should be noted that the efficiency values represented in Fig. 4 are a little too low in comparison with the maximum possible value owing to the excessive length of the outlet electrode [1].

The table gives the heat losses through the different parts of the plasmatron for different values of  $a$  and  $I=180$  a,  $G=10$  g·sec<sup>-1</sup>. The table shows that by halving the length of the outlet electrode the efficiency of the plasmatron can be increased by approximately 4%. It is clear also that with increase in the

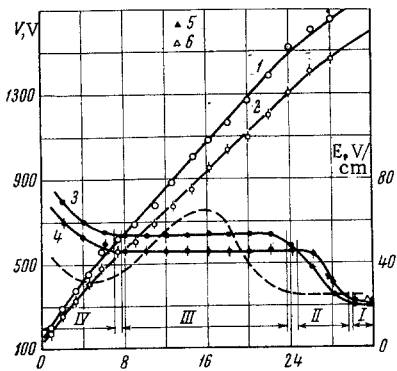


Fig. 7. Distributions of  $V$  (curves 1, 2) and  $E$  (curves 3, 4) in insert region,  $a=33$  cm;  $G=15$  g·sec<sup>-1</sup>;  $I=100$  a for curves 1, 3 and point 5;  $I=170$  a for curves 2, 4 and point 6.

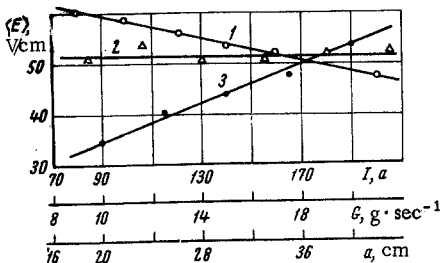


Fig. 8. Mean field of arc in insert region in relation to current (curve 1 for  $a=33$ ,  $G=16$ ), insert length (curve 2 for  $I=100$ ,  $G=15$ ), and air-flow rate (curve 3 for  $I=180$ ,  $a=33$ ).

insert length the heat loss through it increases and the plasmatron efficiency is determined mainly by this loss.

**3. Potential and Electric Field Distributions.** The potential distribution was determined by measuring the potentials of the insulated insert sections, which acquire the arc potential due to an independent discharge between the arc and the wall of the insert section through a layer of relatively cold gas. The method of such measurements was fully described in [3, 4].

Figures 5 and 6 show the results of measurements on the plasmatron in Fig. 1a. The distance from the inside face of the cathode 2 to the considered cross section along the channel axis is plotted on the  $z$  axis (Fig. 1a). The cathode potential is taken as zero.

In [4] a linear relationship was obtained between  $V$  and  $z$  at small  $z$ . In this work we investigated the distribution in a wider range of  $z$  and, as distinct from the results in [4], there are distinctly nonlinear regions. The nonlinearity is particularly distinct close to the cathode and at a certain distance from the anode. The same figures show the distributions of the axial component of the electrode field in the arc in the insert region. The distributions of  $E$  were obtained by differentiation of the curve  $V(z)$  with respect to  $z$ . The obtained data show that  $E$  increases with increase in flow rate.

Figure 7 shows the distribution of  $E$  for an arc in a plasmatron with an inside end-face electrode. It is clearly seen that there are four characteristic regions of variation of  $E$  with  $z$ .

**Region I.** This region was investigated in [4]. The formula given in [4] for calculation of the electric field was

$$E = - G^{0.15} (5160 - 14.8 + 0.073^2) \quad (3.1)$$

where

$$[E] = \text{V}\cdot\text{cm}^{-1}, [G] = \text{kg}\cdot\text{sec}^{-1}, d = 0.01 \text{ m.}$$

The characteristic feature of this region is that  $E$  is independent of  $z$ . Points 5 and 6 were determined from Eq. (3.1). As can be seen, Eq. (3.1) agrees well with the values of  $E$  obtained here.

A comparison of the data of [4] in Fig. 7 shows that the presence of a distributed gas feed greatly reduces the length of region I. This is probably due to the additional turbulation of the flow in the channel by the gas streams flowing in through the gaps between the sections and the presence of annular slits. Confirmation of this hypothesis will reveal a new means of controlling the properties of the arc by artificial alteration of the turbulence of the gas flow.

**Region II.** The characteristic feature of this region is the increase in electric field in the direction of the gas flow. According to Dautov and Sazonov's hypothesis, this increase in  $E(z)$  is due to the characteristic distribution of turbulent transfer coefficients over the radius of the electrode channel and the increase in the arc radius in the downstream direction. In addition, in this case an increase in  $E(z)$  is due to the increase in air flow rate in the direction of the air flow. It should be noted that in regions I and II  $E(z)$  increases with increase in  $I$  when  $I > 100$  a.

**Region III.** The characteristic feature of this region is that  $E$  is independent of  $z$ . This constancy is accompanied by a gradual increase in gas flow rate in the direction of the gas flow. In the absence of a distributed feed in this region there would presumably be a reduction of  $E$  in the direction of the gas flow. As distinct from regions I and II,  $E$  decreases with increase in  $I$  in the current range 80–200 a.

In long arcs the region of the arc corresponding to region III in Fig. 7 is the longest. The main characteristics of the arc will obviously be determined by this region. In particular, the descending U-I characteristics of the plasmatron are the result of the descending E-I characteristics of the arc in region III.

Region IV: The characteristic feature of this region is the increase in E in the direction of the gas flow. The large value of E in this region was attributed in [5] to the effect of the magnetic field proper and rotation of the end of the arc.

In this case, however, there is the additional effect of the external magnetic field produced by solenoid 5 (Fig. 1a).

The same characteristic regions are features of the distributions of E shown in Figs. 5 and 6 for a plasmatron with an inside hollow electrode. The slight difference is due solely to the fact that region I is practically inside the anode and, hence, has little effect on the presented graphs.

As the graphs show, a reduction of the insert length leads to a reduction in the length of region III, whereas the lengths of the other regions are practically unchanged. With short inserts region III is absent and regions II and IV overlap (Fig. 5).

The results given above suggest the following qualitative picture of the change in E (z) in the direction of the gas flow for the case of constant rate of gas flow along the channel. In the initial region E is constant, then increases in the direction of the gas flow, reaches a maximum, decreases, and then increases again in the region subject to the action of the rotating end of the arc (dashed line in Fig. 7).

One other characteristic feature of the arc in the investigated plasmatron with an insert should be mentioned. The mean electric field in the arc in the insert region is independent of the insert length, increases with increase in flow rate, and decreases with increase in current in the range 80-200 a (Fig. 8). In the investigated range of parameters the mean field strength is 30-60 V · cm<sup>-1</sup>, which greatly exceeds the values given in [4] for the field strength for a short arc in a channel without a distributed gas feed.

The author thanks G. Yu. Dautov, M. F. Zhukov, and Yu. S. Dudnikov for useful discussion and constant interest in this work.

#### LITERATURE CITED

1. G. Yu. Dautov, Yu. S. Dudnikov, M. F. Zhukov, G. M. Mustafin, and M. I. Sazonov, "Characteristics of a plasmatron with an interelectrode insert," PMTF [Journal of Applied Mechanics and Technical Physics], No. 1, 1967.
2. G. Yu. (Ju.) Dautov, S. Yu. (Ju) Dudnikov, M. F. Zhukov, and G. M. Mustafin, "Investigation of stabilized arc in the gas flow channel," Eighth International Conference on Phenomena in Ionized Gases, Vienna, 1967.
3. G. Yu. Dautov, Yu. S. Dudnikov, and M. I. Sazonov, "Investigation of a plasmatron with an interelectrode insert," Izv. SO AN SSSR, No. 10, Series 3, 1965.
4. G. Yu. Dautov, Yu. S. Dudnikov, M. I. Sazonov, and M. F. Zhukov, "Potential distribution along the arc in a vortex-stabilized plasma-generator," PMTF [Journal of Applied Mechanics and Technical Physics], No. 5, 1965.
5. A. S. An'shakov, G. Yu. Dautov, G. M. Mustafin, and A. P. Petrov, "An investigation of pulsations in a plasmatron with a self-adjusting arc," PMTF, [Journal of Applied Mechanics and Technical Physics], No. 1, 1967.